

Finding the missing baryons in the intergalactic medium with localized fast radio bursts

K. B. YANG,¹ Q. WU,¹ AND F. Y. WANG^{1,2}

¹*School of Astronomy and Space Science, Nanjing University, Nanjing 210093, China*

²*Key Laboratory of Modern Astronomy and Astrophysics (Nanjing University), Ministry of Education, Nanjing 210093, China*

ABSTRACT

The missing baryon problem is one of the major unsolved problems in astronomy. Fast radio bursts (FRBs) are bright millisecond pulses with unknown origins. The dispersion measure of FRBs is defined as the electron column density along the line of sight, and accounts for every ionized baryon. Here we measure the baryon content of the Universe using 22 localized FRBs. Unlike previous works that fixed the value of dispersion measure of FRB host galaxies and ignored the inhomogeneities of the intergalactic medium (IGM), we use the probability distributions of dispersion measures contributed by host galaxies and IGM from the state-of-the-art IllustrisTNG simulations. We derive the cosmic baryon density of $\Omega_b = 0.0490^{+0.0036}_{-0.0033}$ (1σ), with a precision of 7.0%. This value is dramatically consistent with other measurements, such as the cosmic microwave background and Big Bang nucleosynthesis. Our work supports that the baryons are not missing, but residing in the IGM.

Keywords: Fast Radio Bursts, intergalactic medium

1. INTRODUCTION

The observation of cosmic microwave background (CMB) by Planck Collaboration shows that more than 95% of our universe is composed of dark energy and dark matter, while the rest part of less than 5% is baryonic matter (Planck Collaboration et al. 2020). In the late-time Universe, approximately 17% of the expected baryons are observed to reside in the collapsed phase (Fukugita et al. 1998), including galaxies, groups, and clusters. Numerical simulations (Cen & Ostriker 1999) and observations (Fukugita & Peebles 2004) are performed to study the baryon distribution. However, the fraction of baryons observed in the photoionized Ly α forest and warm-hot intergalactic medium (WHIM) traced by highly ionized states oxygen is only about 53%, which left a vacancy of about 30% (Shull et al. 2012). In recent years, some baryons are found in various ways. de Graaff et al. (2019) found additional $11 \pm 7\%$ baryons with the Sunyaev-Zel'dovich effect from filaments, and the still missing fraction became $18 \pm 16\%$. Some missing baryons had been found in the warm-hot intergalactic medium (Nicastro et al. 2018). Most missing baryons may be residing in diffuse IGM,

which is too faint to detect (McQuinn 2016). Finding the missing baryon is important for us to understand many crucial problems, such as galaxy evolution.

Fast radio bursts (FRBs) are bright millisecond pulses (Petroff et al. 2019; Cordes & Chatterjee 2019; Xiao et al. 2021). Since the first burst, FRB 010724 was discovered in 2007 (Lorimer et al. 2007), over 600 FRBs have been detected (CHIME/FRB Collaboration et al. 2021). When FRBs travel through cold plasma, there will be a time difference between their components of different frequencies, which can be used to define the dispersion measure (DM). DM is defined as the integral of free electron number density along the line of sight. Owing to their large DM in excess of the Galactic value, they are suggested to be extragalactic or cosmological. It is estimated that the majority of DM contribution comes from IGM. The IGM is comprised of highly ionized plasma, which means that the baryon density can be derived from the electron density. Based on the average DM- z relation, short timescales and cosmological origin make them a powerful probe to study the universe and fundamental physics, including measuring Hubble constant (Li et al. 2018; Wu et al. 2022; Hagstotz et al. 2022; James et al. 2022) and Hubble parameter (Wu et al. 2020), measuring cosmic proper distance (Yu & Wang 2017), measuring dark energy (Zhou et al. 2014; Walters et al. 2018; Qiu et al. 2022), bounding the photon rest mass (Wang et al. 2021), measuring reionization history (Zheng et al. 2014; Zhang et al. 2021), testing the weak equivalence principle (Wei et al. 2015), probing compact dark matter (Muñoz et al. 2016; Wang & Wang 2018), and finding “missing” baryons (McQuinn 2014; Walters et al. 2018, 2019; Macquart et al. 2020; Li et al. 2020; Dai & Xia 2021; Wang & Wei 2022). Macquart et al. (2020) performed the first observational constraint on the cosmic baryon density Ω_b using five FRBs, and found $\Omega_b = 0.051_{-0.025}^{+0.021}$ at 95% confidence level, which is consistent with the value derived from the CMB and from Big Bang nucleosynthesis (BBN).

However, there are some obstacles in practice with cosmological applications of FRBs. First, the number of FRBs with measured redshifts is too small, which can be improved with increasing localized FRBs. Thanks to the high event rate, i.e., $10^3 - 10^4$ per day all sky (Thornton et al. 2013; Caleb et al. 2016), the increasing advanced telescopes will localize more FRBs. The second one is that we know little about DM_{host} , the DM contribution from the host galaxy. It is also degenerated with DM_{IGM} , the DM contribution from IGM. How to model DM_{host} is a crucial problem. Third, the IGM inhomogeneity causes the fluctuations of DM_{IGM} along different lines of sight. From cosmological simulations, the variance around the mean DM_{IGM} can be up to 70% (McQuinn 2014; Pol et al. 2019; Zhang et al. 2021). In most previous works, the value of DM_{host} for all host galaxies is treated as a constant, and the fluctuations of DM_{IGM} are ignored. A more appropriate method to describe DM_{IGM} and DM_{host} is needed in the cosmological application of FRBs.

In this letter, we measure the cosmic baryon density with 22 localized FRBs through the DM- z relation. Unlike previous works which assume the DM_{host} as a constant, we use the probability distributions of it from the state-of-the-art IllustrisTNG simulations (Zhang et al. 2020). The effect of different properties of host galaxies on DM_{host} is also taken into consideration. Meanwhile, the fluctuations of DM_{IGM} along different lines of sight are also taken into account (Zhang et al. 2021).

The letter is organized as follows. In section 2, we introduce the probability distributions of DM_{host} and DM_{IGM} , and the method to derive Ω_b . In section 3, we constrain the value of Ω_b through the Monte Carlo Markov Chain (MCMC) analysis. Discussion and conclusions are given in section 4.

2. METHOD

The observed DM of FRBs can be divided into four parts

$$\text{DM}_{\text{obs}} = \text{DM}_{\text{MW}} + \text{DM}_{\text{halo}} + \text{DM}_{\text{IGM}} + \frac{\text{DM}_{\text{host}}}{1+z}, \quad (1)$$

where DM_{MW} is contributed by the interstellar medium of the Milky Way, DM_{halo} is contributed by the Milky Way halo, and DM_{IGM} refers to the contribution of IGM, and DM_{host} is contributed by the host galaxy. For the first part DM_{MW} , some models have been built, including NE2001 and YMW16 models (Cordes & Lazio 2002; Yao et al. 2017). In this work, we use the NE2001 model to estimate the value of DM_{MW} . After deducing the DM_{MW} from DM_{obs} , we can get $\text{DM}'_{\text{FRB}} = \text{DM}_{\text{IGM}} + \text{DM}_{\text{host}} + \text{DM}_{\text{halo}}$. Only the part DM_{IGM} contains the cosmological information, including the cosmic baryon density Ω_b . However, it's difficult to separate it from DM_{host} and DM_{halo} , which is the key point for the cosmological applications of FRBs. Besides, due to the matter inhomogeneity in the IGM and the diverse properties of host galaxies, both of them can not be accurately determined.

In a flat Λ CDM universe, the average DM_{IGM} is (Deng & Zhang 2014; Macquart et al. 2020)

$$\langle \text{DM}_{\text{IGM}} \rangle = \frac{3c\Omega_b H_0}{8\pi G m_p} \int_0^{z_{\text{FRB}}} \frac{f_{\text{IGM}}(z) f_e(z) (1+z)}{\sqrt{\Omega_m (1+z)^3 + \Omega_\Lambda}} dz, \quad (2)$$

where m_p is the rest proton mass, Ω_m is the cosmic matter density, and the electron fraction is $f_e(z) = Y_H X_{e,H}(z) + \frac{1}{2} Y_{He} X_{e,He}(z) = 7/8$. For a flat universe, $\Omega_m = 1 - \Omega_\Lambda$. $f_{\text{IGM}}(z)$ is the fraction of baryons in the IGM. At present, we know little about the evolution model of $f_{\text{IGM}}(z)$ with redshift z . $f_{\text{IGM}}(z)$ could increase with redshifts as massive halos grow abundant with the universe evolving. It's estimated that the value of f_{IGM} is 0.82 at low redshifts and 0.9 at $z > 1.5$ (Meiksin 2009; Shull et al. 2012). For the Hubble constant H_0 , a fiducial value of 70 km/s/Mpc is used.

As mentioned above, it is difficult to determine the exact value of DM_{halo} , DM_{host} and DM_{IGM} . So we focus on the probability distributions of them. The DM_{halo} contributed by the halo is estimated to be $50 \sim 80 \text{ pc cm}^{-3}$ (Prochaska & Zheng 2019). According to this estimation, we assume that the distribution of DM_{halo} is a Gaussian distribution with the standard deviation $\sigma_{\text{halo}} = 15 \text{ pc cm}^{-3}$ and the mean value $\mu_{\text{halo}} = 65 \text{ pc cm}^{-3}$ (Wu et al. 2022), i.e.,

$$P_{\text{halo}}(\text{DM}_{\text{halo}} | \mu_{\text{halo}}, \sigma_{\text{halo}}) = \frac{1}{\sigma_{\text{halo}} \sqrt{2\pi}} \exp\left[-\frac{(\text{DM}_{\text{halo}} - \mu_{\text{halo}})^2}{2\sigma_{\text{halo}}^2}\right]. \quad (3)$$

It is worth noting that DM_{halo} is larger than 30 pc cm^{-3} , and should be smaller than 100 pc cm^{-3} for FRBs at high galactic latitudes and longitudes (Yamasaki & Totani 2020). Positions of FRBs with known coordinates are shown in figure 1. All of them satisfy this condition. For conservative estimations, the range of DM_{halo} is adopted as $30 \sim 100 \text{ pc cm}^{-3}$ in our calculation (Yamasaki & Totani 2020).

For localized FRBs, we can calculate the average $\langle \text{DM}_{\text{IGM}} \rangle$ with equation (2). The probability distribution of DM_{IGM} can be described as a long-tailed quasi-Gaussian function of the average value (McQuinn 2014; Macquart et al. 2020; Zhang et al. 2021),

$$P_{\text{IGM}}(\Delta) = A \Delta^{-\beta} \exp\left[-\frac{(\Delta^{-\alpha} - C_0)^2}{2\alpha^2 \sigma_{\text{DM}}^2}\right], \Delta > 0, \quad (4)$$

where $\Delta = \text{DM}_{\text{IGM}} / \langle \text{DM}_{\text{IGM}} \rangle$, α and β are related to profile scales and their best fits are $\alpha = 3$ and $\beta = 3$ (Macquart et al. 2020). σ_{DM} is the effective deviation caused by the inhomogeneities of IGM.

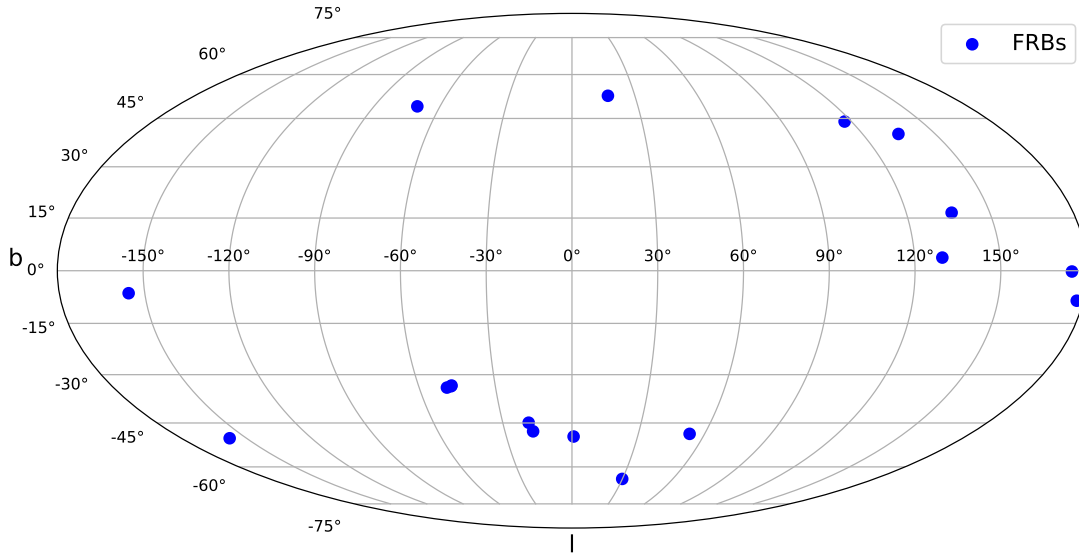


Figure 1. The coordinates of 18 localized FRBs in the galactic coordinate system. There is no FRB with both low galactic latitudes and low galactic longitudes.

Zhang et al. (2021) have given the best fits of C_0 , A and σ_{DM} at several different redshifts derived from the IllustrisTNG simulation. These redshifts do not include the redshifts of the FRBs used in this work. Using the cubic spline interpolation method, we get C_0 , A and σ_{DM} as a function of redshift. Then, the values of C_0 , A and σ_{DM} at given redshifts are derived.

A log-normal function can well describe the distribution of DM_{host} (Macquart et al. 2020; Zhang et al. 2020),

$$P_{\text{host}}(DM_{\text{host}}|\mu, \sigma) = \frac{1}{DM_{\text{host}}\sigma\sqrt{2\pi}}\exp\left[-\frac{(\ln DM_{\text{host}} - \mu)^2}{2\sigma^2}\right], \quad (5)$$

where μ and σ are free parameters. For this distribution, the expected value and standard deviation are e^μ and $e^{2\mu+\sigma^2}[e^{\sigma^2} - 1]$, respectively. Zhang et al. (2020) have given the best fitting values of μ and σ through the state-of-the-art IllustrisTNG simulations. In their work, FRBs are divided into three types according to the observational properties of host galaxies: repeating FRBs like FRB 121102 (Type I), repeating FRBs like FRB 180916 (Type II) and non-repeating FRBs (Type III). Repeating bursts may originate from newborn neutron stars (Wang et al. 2020). FRB 121102 is localized to a dwarf galaxy with a low star formation rate, hence repeating FRBs like FRB121102 may be from dwarf galaxies with low metallicity (Chatterjee et al. 2017). The host galaxy of FRB 180916 is a spiral galaxy, which is different from that of FRB 121102. It was born in a star-forming region (Marcote et al. 2020). Therefore repeating FRBs like FRB 180916 are likely to reside in the star-forming region. Non-repeating FRBs may originate from the merger of compact binaries (Totani 2013; Wang et al. 2016), and their locations are far from the galaxy centers (Bannister et al. 2019; Prochaska et al. 2019). In our calculation, as before, we use their results to get μ and σ at given redshifts by cubic spline interpolation.

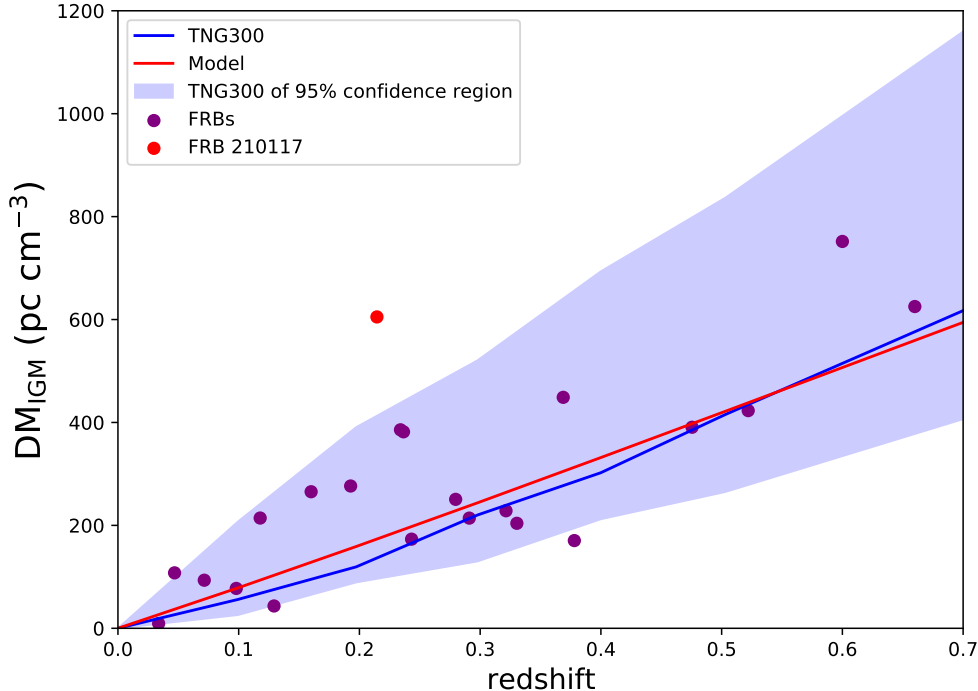


Figure 2. The $DM_{\text{IGM}} - z$ relation for FRBs. The scatter star points are 23 localized FRBs. DM_{IGM} values are derived by deducing the DM_{MW} , DM_{halo} and DM_{host} from DM_{obs} . DM_{MW} values are deduced from NE2001 model, and DM_{halo} values are estimated to be 65 pc cm^{-3} . We use the median value of DM_{host} at different redshifts according to equation (5). The blue line is the result derived from IllustrisTNG 300 cosmological simulation and the green shaded region is the 95% confidence level. The red line represents the theoretical model DM_{IGM} (equation (2)) assuming $f_{\text{IGM}} = 0.82$, $\Omega_b = 0.0488$ and $H_0 = 70 \text{ km s}^{-1} \text{ Mpc}^{-1}$. Due to FRB 210117 deviates from the 95% confidence region of DM_{IGM} , we exclude it in the following analysis.

For an FRB with a given redshift z and $DM'_{\text{FRB},i}$, we can calculate the total probability density function (PDF) through

$$P_i(DM'_{\text{FRB},i} | z_i) = \int_{30}^{100} \int_0^{DM'_{\text{FRB},i} - DM_{\text{halo}}} P_{\text{IGM}}(DM_{\text{IGM}}) P_{\text{halo}}(DM_{\text{halo}} | \mu_{\text{halo}}, \sigma_{\text{halo}}) P_{\text{host}}(DM'_{\text{FRB},i} - DM_{\text{IGM}} - DM_{\text{halo}} | \mu, \sigma_{\text{host}}) dDM_{\text{IGM}} dDM_{\text{halo}}. \quad (6)$$

At last, we obtain the joint likelihood function by multiplying the PDF of each FRB

$$\mathcal{L} = \prod_{i=1}^{N_{\text{FRB}}} P_i(DM'_{\text{FRB},i} | z_i). \quad (7)$$

3. DATA AND RESULTS

Though over 600 FRBs have been observed, only 24 of them have been localized. 19 of them are collected at <http://frbhosts.org/#explore>, including the nearest one FRB 20200120E. This FRB is

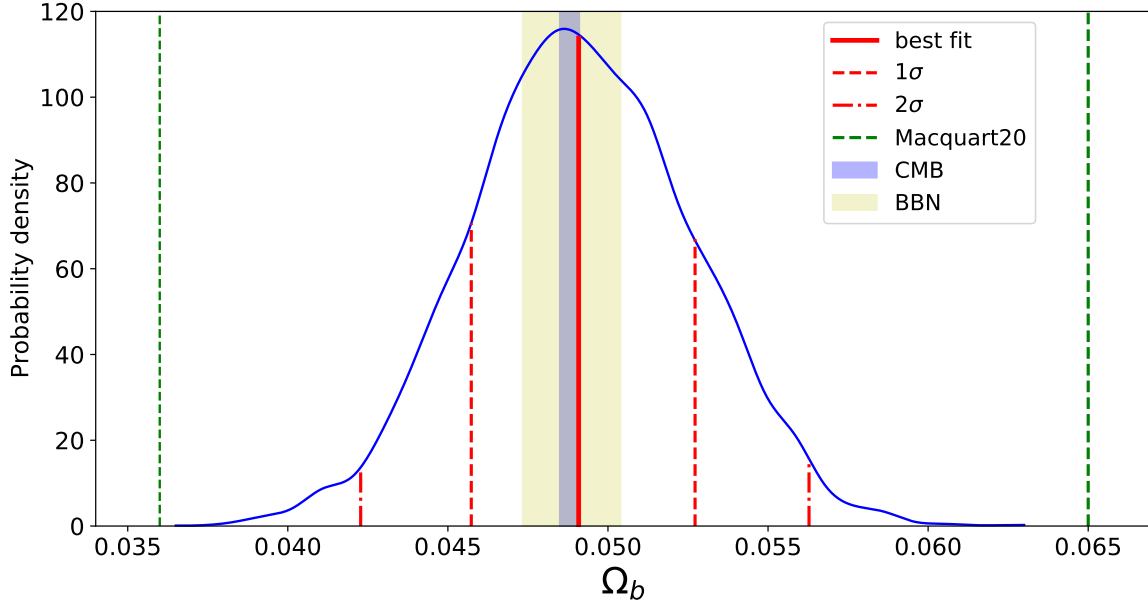


Figure 3. The normalized probability density distribution of Ω_b from 22 localized FRBs. The best fit is $\Omega_b = 0.0490^{+0.0036}_{-0.0033}$ in 1σ confidence level. The red solid line shows the best-fit value, and dotted lines present the 1σ and 2σ confidence levels. The blue shade region shows the constraint on Ω_b from CMB with 1σ confidence level, and the yellow shade region represents the constraint from BBN with 1σ confidence level. The green dashed lines correspond to the 1σ uncertainty range of Ω_b derived by [Macquart et al. \(2020\)](#).

localized in a globular cluster in M81, whose distance is only 3.6 Mpc ([Bhardwaj et al. 2021a](#); [Kirsten et al. 2021](#)). It is obvious that it contains little cosmological information and we exclude it. The other five FRBs localized by the Australian Square Kilometre Array Pathfinder (ASKAP) are given in [James et al. \(2022\)](#). The parameters of all 23 localized FRBs are shown in Table 1. It lists the redshifts, DM_{obs} , $DM_{\text{MW,ISM}}$, host type and references of them. In figure 2, we plot the $DM_{\text{IGM}} - z$ relation of 23 localized FRBs. The derived DM_{IGM} of FRBs are shown as scatters. The red line shows the averaged value of DM_{IGM} from the equation (2). The blue line is the DM_{IGM} estimated from the IllustrisTNG simulation with 95% confidence region ([Zhang et al. 2021](#)). FRB 210117 deviates from the 95% confidence region, which may be caused by the DM contributed by the plasma near the FRB source, similar as that of FRB 190520B ([Zhao & Wang 2021](#); [Katz 2022](#)). Therefore, we exclude this FRB in the following analysis. We use the NE2001 model to calculate the DM contribution by the ISM of Milky Way ([Cordes & Lazio 2002](#)).

The MCMC Python module *emcee* is used to estimate Ω_b ([Foreman-Mackey et al. 2013](#)). Ω_m and H_0 are also free parameters to be fitted in our analysis. Cosmological observations have tightly constrained them. As shown in below, they have little effect on the final constraints on Ω_b . The steps of MCMC analysis are as follows.

(a) Firstly, we get the $(DM_{\text{FRB}'}, z)$ dataset by deducing the DM_{MW} obtained from the NE2001 model from DM_{obs} . Then we calculate the probability density of $DM_{\text{FRB}'}$ for each FRB using equations (3), (4), (5) and (6). The joint likelihood function is obtained by multiplying the PDF of each FRB with equation (7).

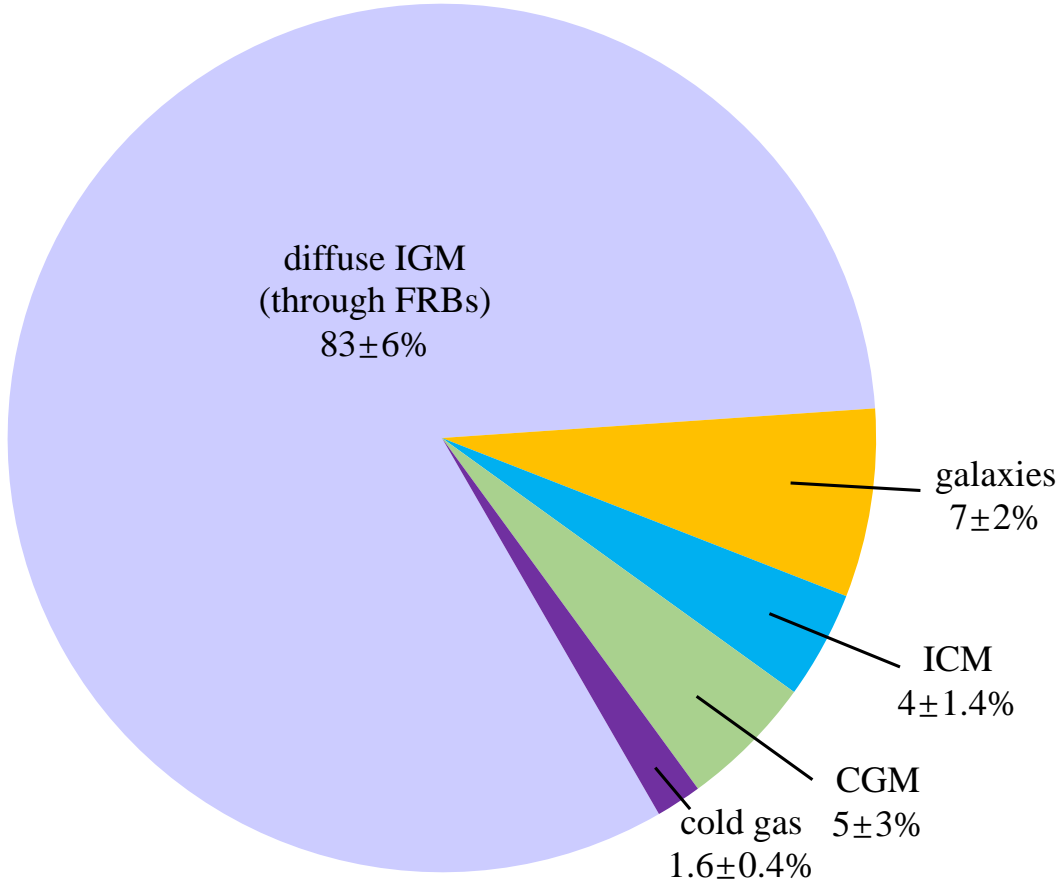


Figure 4. Current observational measurements of the low redshift baryon census. From the DM– z relation of FRBs, $83\% \pm 6\%$ of the cosmic baryons in the diffuse form are derived. The values in collapsed forms, including in galaxies, the CGM, the ICM, and cold gas, are adjusted from Shull et al. (2012). Collapsed phases (galaxies, CGM, ICM, and cold neutral gas) contribute $17\% \pm 4\%$ of the total cosmic baryons. From our study, almost 100% cosmic baryons are found in the late-time Universe.

(b) Next, we need to set the priors for the parameters to be fit. For Ω_b , we assume a uniform prior of range [0.03, 0.065]. H_0 and Ω_b are also set priors to estimate their impact. For the Hubble constant H_0 , the measurements of H_0 , from SNe Ia and CMB, are mainly distributed between $67 \text{ km s}^{-1}\text{Mpc}^{-1}$ and $73 \text{ km s}^{-1}\text{Mpc}^{-1}$ (Planck Collaboration et al. 2020; Riess et al. 2022). Therefore, we assume a uniform prior of range [67, 73] $\text{km s}^{-1}\text{Mpc}^{-1}$. A fiducial value of $H_0=70 \text{ km/s/Mpc}$ is used by Macquart et al. (2020). Finally, we assume a uniform prior of [0.28, 0.35] for Ω_m because most of the measurements of Ω_m are in this range (Brout et al. 2022; Scolnic et al. 2018).

(c) At last, we run 10000 steps of MCMC using Python package emcee with the likelihood function equation 7. The result is $\Omega_b = 0.0490^{+0.0036}_{-0.0033}$ (1σ) with a 7.0% precision. This value is consistent with previous results in 1σ confidence level, such as CMB and BBN (Planck Collaboration et al. 2020; Cooke et al. 2018). Macquart et al. (2020) used five FRBs to constrain Ω_b , and found $\Omega_b = 0.051^{+0.021}_{-0.025}$ with 95 percent confidence by assuming $H_0=70 \text{ km/s/Mpc}$. This value is compatible with our result in 1σ confidence level, but with large error.

In the calculation, the fraction of baryons in the IGM $f_{\text{IGM}} = 0.82$ is used. It must be noted that Ω_b and f_{IGM} are degenerated. In fact, only the product of Ω_b , H_0 and f_{IGM} can be derived. Conversely,

if the value of Ω_b from CMB is fixed, the constraint on f_{IGM} should be close to 0.82. The same prior for H_0 and the best constraint on Ω_b from CMB are used. Using the method as above, we derive $f_{\text{IGM}} = 0.83 \pm 0.06$.

Figure 4 shows the current census of baryons in the low-redshift Universe, including diffuse form revealed by FRBs, and collapsed forms. Collapsed forms contain galaxies, the circumgalactic medium (CGM), intercluster medium (ICM), and cold neutral gas (H I and He I). These slices show the contributions, $\Omega_b^i/\Omega_{\text{tot,b}}$ to the total baryon content from components i . Previous studies found that $5\% \pm 3\%$ may reside in circumgalactic gas, $7\% \pm 2\%$ in galaxies, $1.7\% \pm 0.4\%$ in cold gas and $4\% \pm 1.4\%$ in clusters (Shull et al. 2012). From our analysis, the measurement of FRBs can account for $83\% \pm 6\%$ of the baryons in the Universe. Therefore, the missing baryons are found in the IGM through localized FRBs.

4. DISCUSSION AND CONCLUSIONS

The statistical and systematic errors must be taken into consideration. The statistical error refers to the small number of localized FRBs. As mentioned above, this will be improved with the increase of localized FRBs. The systematic error includes all the uncertainties except statistical errors, such as cosmological parameters, observational errors of DM and redshift. It cannot be eliminated by more data. More precise measurements of these parameters are needed. Besides, YMW16 model gives a larger DM_{MW} value than the NE2001 model. This may lead to a similar but smaller result.

In equation (4), the best-fit parameters for C_0 , σ_{DM} and A are taken from Zhang et al. (2021). Their uncertainties may affect the final Ω_b constraint. We derive their uncertainties from the original data. From equations (4) (6) and (7), it is obvious that the uncertainty of A has no effect on the result. To consider the effect of C_0 and σ_{DM} , we derive Ω_b using the best-fit values of C_0 and σ_{DM} plus or minus the uncertainties respectively, totaling four probability distributions of DM_{IGM} . The results of fits are $\Omega_b = 0.0492^{+0.0035}_{-0.0034}$, $0.0492^{+0.0035}_{-0.0034}$, $0.0481^{+0.0036}_{-0.0034}$ and $0.0493^{+0.0036}_{-0.0033}$ in these four case. These constraints are very close to the original result (approximately 0.25σ) and their errors are almost the same. Therefore we can conclude that uncertainties of C_0 , σ_{DM} and A have almost no effect on final Ω_b constraint. Besides, our calculation is not entirely independent of cosmological parameters, such as Ω_m and H_0 . We adopt their ranges limited by observations.

In summary, we estimate the cosmic baryon density, Ω_b using 22 localized FRBs by considering the probability distributions of DMs contributed by host galaxies and IGM. We obtain the result $\Omega_b = 0.0492^{+0.0035}_{-0.0034}$ (1σ) with a 7.0% precision. The result is consistent with those derived from CMB and BBN. So, FRBs can provide an independent measurement of Ω_b with high precision. Our work shows that the missing baryons are found in diffuse IGM by FRBs.

ACKNOWLEDGEMENTS

We thank the anonymous referee for helpful comments. This work was supported by the National Natural Science Foundation of China (grant Nos. U1831207 and 12273009), the National Key Research and Development Program of China (2022SKA0130100), the Fundamental Research Funds for the Central Universities (No. 0201-14380045) and the China Manned Space Project (CMS-CSST-2021-A12).

REFERENCES

- | | |
|---|--|
| Bannister, K. W., Deller, A. T., Phillips, C., et al.
2019, <i>Science</i> , 365, 565,
doi: 10.1126/science.aaw5903 | Bhandari, S., Sadler, E. M., Prochaska, J. X.,
et al. 2020, <i>ApJL</i> , 895, L37,
doi: 10.3847/2041-8213/ab672e |
|---|--|

- Bhandari, S., Heintz, K. E., Aggarwal, K., et al. 2021, arXiv e-prints, arXiv:2108.01282. <https://arxiv.org/abs/2108.01282>
- Bhardwaj, M., Gaensler, B. M., Kaspi, V. M., et al. 2021a, ApJL, 910, L18, doi: [10.3847/2041-8213/abeaa6](https://doi.org/10.3847/2041-8213/abeaa6)
- Bhardwaj, M., Kirichenko, A. Y., Michilli, D., et al. 2021b, ApJL, 919, L24, doi: [10.3847/2041-8213/ac223b](https://doi.org/10.3847/2041-8213/ac223b)
- Brout, D., Scolnic, D., Popovic, B., et al. 2022, ApJ, 938, 110, doi: [10.3847/1538-4357/ac8e04](https://doi.org/10.3847/1538-4357/ac8e04)
- Caleb, M., Flynn, C., Bailes, M., et al. 2016, MNRAS, 458, 718, doi: [10.1093/mnras/stw109](https://doi.org/10.1093/mnras/stw109)
- Cen, R., & Ostriker, J. P. 1999, ApJ, 514, 1, doi: [10.1086/306949](https://doi.org/10.1086/306949)
- Chatterjee, S., Law, C. J., Wharton, R. S., et al. 2017, Nature, 541, 58, doi: [10.1038/nature20797](https://doi.org/10.1038/nature20797)
- CHIME/FRB Collaboration, Amiri, M., Andersen, B. C., et al. 2021, ApJS, 257, 59, doi: [10.3847/1538-4365/ac33ab](https://doi.org/10.3847/1538-4365/ac33ab)
- Chittidi, J. S., Simha, S., Mannings, A., et al. 2021, ApJ, 922, 173, doi: [10.3847/1538-4357/ac2818](https://doi.org/10.3847/1538-4357/ac2818)
- Cooke, R. J., Pettini, M., & Steidel, C. C. 2018, ApJ, 855, 102, doi: [10.3847/1538-4357/aaab53](https://doi.org/10.3847/1538-4357/aaab53)
- Cordes, J. M., & Chatterjee, S. 2019, ARA&A, 57, 417, doi: [10.1146/annurev-astro-091918-104501](https://doi.org/10.1146/annurev-astro-091918-104501)
- Cordes, J. M., & Lazio, T. J. W. 2002, arXiv e-prints, astro. <https://arxiv.org/abs/astro-ph/0207156>
- Dai, J.-P., & Xia, J.-Q. 2021, MNRAS, 503, 4576, doi: [10.1093/mnras/stab785](https://doi.org/10.1093/mnras/stab785)
- Day, C. K., Deller, A. T., Shannon, R. M., et al. 2020, MNRAS, 497, 3335, doi: [10.1093/mnras/staa2138](https://doi.org/10.1093/mnras/staa2138)
- de Graaff, A., Cai, Y.-C., Heymans, C., & Peacock, J. A. 2019, A&A, 624, A48, doi: [10.1051/0004-6361/201935159](https://doi.org/10.1051/0004-6361/201935159)
- Deng, W., & Zhang, B. 2014, ApJL, 783, L35, doi: [10.1088/2041-8205/783/2/L35](https://doi.org/10.1088/2041-8205/783/2/L35)
- Fong, W.-f., Dong, Y., Leja, J., et al. 2021, ApJL, 919, L23, doi: [10.3847/2041-8213/ac242b](https://doi.org/10.3847/2041-8213/ac242b)
- Foreman-Mackey, D., Hogg, D. W., Lang, D., & Goodman, J. 2013, PASP, 125, 306, doi: [10.1086/670067](https://doi.org/10.1086/670067)
- Fukugita, M., Hogan, C. J., & Peebles, P. J. E. 1998, ApJ, 503, 518, doi: [10.1086/306025](https://doi.org/10.1086/306025)
- Fukugita, M., & Peebles, P. J. E. 2004, ApJ, 616, 643, doi: [10.1086/425155](https://doi.org/10.1086/425155)
- Hagstotz, S., Reischke, R., & Lilow, R. 2022, MNRAS, 511, 662, doi: [10.1093/mnras/stac077](https://doi.org/10.1093/mnras/stac077)
- Heintz, K. E., Prochaska, J. X., Simha, S., et al. 2020, ApJ, 903, 152, doi: [10.3847/1538-4357/abb6fb](https://doi.org/10.3847/1538-4357/abb6fb)
- James, C. W., Ghosh, E. M., Prochaska, J. X., et al. 2022, arXiv e-prints, arXiv:2208.00819. <https://arxiv.org/abs/2208.00819>
- Katz, J. I. 2022, MNRAS, 510, L42, doi: [10.1093/mnras/slab128](https://doi.org/10.1093/mnras/slab128)
- Kirsten, F., Marcote, B., Nimmo, K., et al. 2021, arXiv e-prints, arXiv:2105.11445. <https://arxiv.org/abs/2105.11445>
- Law, C. J., Butler, B. J., Prochaska, J. X., et al. 2020, ApJ, 899, 161, doi: [10.3847/1538-4357/aba4ac](https://doi.org/10.3847/1538-4357/aba4ac)
- Li, Z., Gao, H., Wei, J. J., et al. 2020, MNRAS, 496, L28, doi: [10.1093/mnras/slaa070](https://doi.org/10.1093/mnras/slaa070)
- Li, Z.-X., Gao, H., Ding, X.-H., Wang, G.-J., & Zhang, B. 2018, Nature Communications, 9, 3833, doi: [10.1038/s41467-018-06303-0](https://doi.org/10.1038/s41467-018-06303-0)
- Lorimer, D. R., Bailes, M., McLaughlin, M. A., Narkevic, D. J., & Crawford, F. 2007, Science, 318, 777, doi: [10.1126/science.1147532](https://doi.org/10.1126/science.1147532)
- Macquart, J. P., Prochaska, J. X., McQuinn, M., et al. 2020, Nature, 581, 391, doi: [10.1038/s41586-020-2300-2](https://doi.org/10.1038/s41586-020-2300-2)
- Marcote, B., Nimmo, K., Hessels, J. W. T., et al. 2020, Nature, 577, 190, doi: [10.1038/s41586-019-1866-z](https://doi.org/10.1038/s41586-019-1866-z)
- McQuinn, M. 2014, ApJL, 780, L33, doi: [10.1088/2041-8205/780/2/L33](https://doi.org/10.1088/2041-8205/780/2/L33)
- . 2016, ARA&A, 54, 313, doi: [10.1146/annurev-astro-082214-122355](https://doi.org/10.1146/annurev-astro-082214-122355)
- Meiksin, A. A. 2009, Reviews of Modern Physics, 81, 1405, doi: [10.1103/RevModPhys.81.1405](https://doi.org/10.1103/RevModPhys.81.1405)
- Muñoz, J. B., Kovetz, E. D., Dai, L., & Kamionkowski, M. 2016, PhRvL, 117, 091301, doi: [10.1103/PhysRevLett.117.091301](https://doi.org/10.1103/PhysRevLett.117.091301)
- Nicastro, F., Kaastra, J., Krongold, Y., et al. 2018, Nature, 558, 406, doi: [10.1038/s41586-018-0204-1](https://doi.org/10.1038/s41586-018-0204-1)
- Petroff, E., Hessels, J. W. T., & Lorimer, D. R. 2019, A&A Rv, 27, 4, doi: [10.1007/s00159-019-0116-6](https://doi.org/10.1007/s00159-019-0116-6)
- Planck Collaboration, Aghanim, N., Akrami, Y., et al. 2020, A&A, 641, A6, doi: [10.1051/0004-6361/201833910](https://doi.org/10.1051/0004-6361/201833910)

- Pol, N., Lam, M. T., McLaughlin, M. A., Lazio, T. J. W., & Cordes, J. M. 2019, *ApJ*, 886, 135, doi: [10.3847/1538-4357/ab4c2f](https://doi.org/10.3847/1538-4357/ab4c2f)
- Prochaska, J. X., & Zheng, Y. 2019, *MNRAS*, 485, 648, doi: [10.1093/mnras/stz261](https://doi.org/10.1093/mnras/stz261)
- Prochaska, J. X., Macquart, J.-P., McQuinn, M., et al. 2019, *Science*, 366, 231, doi: [10.1126/science.aay0073](https://doi.org/10.1126/science.aay0073)
- Qiu, X.-W., Zhao, Z.-W., Wang, L.-F., Zhang, J.-F., & Zhang, X. 2022, *JCAP*, 2022, 006, doi: [10.1088/1475-7516/2022/02/006](https://doi.org/10.1088/1475-7516/2022/02/006)
- Ravi, V., Catha, M., D’Addario, L., et al. 2019, *Nature*, 572, 352, doi: [10.1038/s41586-019-1389-7](https://doi.org/10.1038/s41586-019-1389-7)
- Riess, A. G., Yuan, W., Macri, L. M., et al. 2022, *ApJL*, 934, L7, doi: [10.3847/2041-8213/ac5c5b](https://doi.org/10.3847/2041-8213/ac5c5b)
- Scolnic, D. M., Jones, D. O., Rest, A., et al. 2018, *ApJ*, 859, 101, doi: [10.3847/1538-4357/aab9bb](https://doi.org/10.3847/1538-4357/aab9bb)
- Shull, J. M., Smith, B. D., & Danforth, C. W. 2012, *ApJ*, 759, 23, doi: [10.1088/0004-637X/759/1/23](https://doi.org/10.1088/0004-637X/759/1/23)
- Spitler, L. G., Scholz, P., Hessels, J. W. T., et al. 2016, *Nature*, 531, 202, doi: [10.1038/nature17168](https://doi.org/10.1038/nature17168)
- Thornton, D., Stappers, B., Bailes, M., et al. 2013, *Science*, 341, 53, doi: [10.1126/science.1236789](https://doi.org/10.1126/science.1236789)
- Totani, T. 2013, *PASJ*, 65, L12, doi: [10.1093/pasj/65.5.L12](https://doi.org/10.1093/pasj/65.5.L12)
- Walters, A., Ma, Y.-Z., Sievers, J., & Weltman, A. 2019, *PhRvD*, 100, 103519, doi: [10.1103/PhysRevD.100.103519](https://doi.org/10.1103/PhysRevD.100.103519)
- Walters, A., Weltman, A., Gaensler, B. M., Ma, Y.-Z., & Witzemann, A. 2018, *ApJ*, 856, 65, doi: [10.3847/1538-4357/aaaf6b](https://doi.org/10.3847/1538-4357/aaaf6b)
- Wang, B., & Wei, J.-J. 2022, arXiv e-prints, arXiv:2211.02209. <https://arxiv.org/abs/2211.02209>
- Wang, F. Y., Wang, Y. Y., Yang, Y.-P., et al. 2020, *ApJ*, 891, 72, doi: [10.3847/1538-4357/ab74d0](https://doi.org/10.3847/1538-4357/ab74d0)
- Wang, H., Miao, X., & Shao, L. 2021, *Physics Letters B*, 820, 136596, doi: [10.1016/j.physletb.2021.136596](https://doi.org/10.1016/j.physletb.2021.136596)
- Wang, J.-S., Yang, Y.-P., Wu, X.-F., Dai, Z.-G., & Wang, F.-Y. 2016, *ApJL*, 822, L7, doi: [10.3847/2041-8205/822/1/L7](https://doi.org/10.3847/2041-8205/822/1/L7)
- Wang, Y. K., & Wang, F. Y. 2018, *A&A*, 614, A50, doi: [10.1051/0004-6361/201731160](https://doi.org/10.1051/0004-6361/201731160)
- Wei, J.-J., Gao, H., Wu, X.-F., & Mészáros, P. 2015, *PhRvL*, 115, 261101, doi: [10.1103/PhysRevLett.115.261101](https://doi.org/10.1103/PhysRevLett.115.261101)
- Wu, Q., Yu, H., & Wang, F. Y. 2020, *ApJ*, 895, 33, doi: [10.3847/1538-4357/ab88d2](https://doi.org/10.3847/1538-4357/ab88d2)
- Wu, Q., Zhang, G.-Q., & Wang, F.-Y. 2022, *MNRAS*, 515, L1, doi: [10.1093/mnrasl/slac022](https://doi.org/10.1093/mnrasl/slac022)
- Xiao, D., Wang, F., & Dai, Z. 2021, *Science China Physics, Mechanics, and Astronomy*, 64, 249501, doi: [10.1007/s11433-020-1661-7](https://doi.org/10.1007/s11433-020-1661-7)
- Yamasaki, S., & Totani, T. 2020, *ApJ*, 888, 105, doi: [10.3847/1538-4357/ab58c4](https://doi.org/10.3847/1538-4357/ab58c4)
- Yao, J. M., Manchester, R. N., & Wang, N. 2017, *ApJ*, 835, 29, doi: [10.3847/1538-4357/835/1/29](https://doi.org/10.3847/1538-4357/835/1/29)
- Yu, H., & Wang, F. Y. 2017, *A&A*, 606, A3, doi: [10.1051/0004-6361/201731607](https://doi.org/10.1051/0004-6361/201731607)
- Zhang, G. Q., Yu, H., He, J. H., & Wang, F. Y. 2020, *ApJ*, 900, 170, doi: [10.3847/1538-4357/abaa4a](https://doi.org/10.3847/1538-4357/abaa4a)
- Zhang, Z. J., Yan, K., Li, C. M., Zhang, G. Q., & Wang, F. Y. 2021, *ApJ*, 906, 49, doi: [10.3847/1538-4357/abceb9](https://doi.org/10.3847/1538-4357/abceb9)
- Zhao, Z. Y., & Wang, F. Y. 2021, *ApJL*, 923, L17, doi: [10.3847/2041-8213/ac3f2f](https://doi.org/10.3847/2041-8213/ac3f2f)
- Zheng, Z., Ofek, E. O., Kulkarni, S. R., Neill, J. D., & Juric, M. 2014, *ApJ*, 797, 71, doi: [10.1088/0004-637X/797/1/71](https://doi.org/10.1088/0004-637X/797/1/71)
- Zhou, B., Li, X., Wang, T., Fan, Y.-Z., & Wei, D.-M. 2014, *PhRvD*, 89, 107303, doi: [10.1103/PhysRevD.89.107303](https://doi.org/10.1103/PhysRevD.89.107303)

Table 1. Properties of localized FRBs

Name	Redshift	DM _{obs} (pc cm ⁻³)	DM _{MW,ISM} (pc cm ⁻³)	Host Type	Reference
FRB 121102	0.19273	557	188.0	I	Spitler et al. (2016)
FRB 180301	0.3304	534	152	I	Bhandari et al. (2021)
FRB 180916	0.0337	348.8	200.0	II	Marcote et al. (2020)
FRB 180924	0.3214	361.42	40.5	III	Bannister et al. (2019)
FRB 181030	0.0039	103.5	41	I	Bhardwaj et al. (2021b)
FRB 181112	0.4755	89.27	102.0	III	Prochaska et al. (2019)
FRB 190102	0.291	363.6	57.3	III	Bhandari et al. (2020)
FRB 190523	0.66	760.8	37.0	III	Ravi et al. (2019)
FRB 190608	0.1178	338.7	37.2	III	Chittidi et al. (2021)
FRB 190611	0.378	321.4	57.8	III	Day et al. (2020)
FRB 190614	0.6	959.2	83.5	III	Law et al. (2020)
FRB 190711	0.522	593.1	56.4	I	Heintz et al. (2020)
FRB 190714	0.2365	504.13	38.0	III	Heintz et al. (2020)
FRB 191001	0.234	507.9	44.7	III	Heintz et al. (2020)
FRB 191228	0.2432	297.5	33	III	Bhandari et al. (2021)
FRB 200430	0.16	380.25	27.0	III	Heintz et al. (2020)
FRB 200906	0.3688	577.8	36	III	Bhandari et al. (2021)
FRB 201124	0.098	413.52	123.2	II	Fong et al. (2021)
FRB 210117	0.2145	730	34.4	III	James et al. (2022)
FRB 210320	0.2797	384.8	42	III	James et al. (2022)
FRB 210807	0.12927	251.9	121.2	III	James et al. (2022)
FRB 211127	0.0469	234.83	42.5	III	James et al. (2022)
FRB 211212	0.0715	206	27.1	III	James et al. (2022)